https://doi.org/10.15407/knit2024.05.003
UDC 629.78

C. WANG[1], Professor
https://orcid.org/0000-0002-1358-7731
E-mail: wangcq@nwpu.edu.cn
A. E. ZAKRZHEVSKII[2], Dr. Sci. in Tech., Leading scientist, Professor
https://orcid.org/0000-0003-2106-2086
E-mail: alex.e.zakr@gmail.com

[1]Department of Navigation, Guidance, and Control, Northwestern Polytechnical University 1
127 Youyi Xilu, Xi'an 710072 Shaanxi, P. R. China
[2] Space Research Institute of National Academy of Sciences of Ukraine and State Space Agency of Ukraine
40, Glushkov Ave., build. 4/1, Kyiv 187, 03680 Ukraine

PROGRAMMED CONTROL OF ADDITIONAL DEPLOYMENT OF A SPACE TETHER WITH RECOVERY OF ITS INITIAL VERTICAL ORIENTATION

The additional deployment of a two-body space tether with a massless cable is studied to develop a feed-forward control by the mode of increasing the length of a previously deployed space tether with the recovery of its initial vertical orientation. The motion equations of the variable length tether, written in spherical coordinates, are used for it. The developed feed-forward control by the length of the tether provides the necessary change of its angular momentum under the effect of the gravitational torque. The novelty of the results consists of developing a new approach to creating control for underactuated mechanical systems, which have a number of control channels less than the number of degrees of freedom. Here, a tether length control is developed, which allows for the control of its motion about the pitch axis, using only one tether length control channel. The passive but controlled effect of the gravitational torque on the tether is used for this purpose. To achieve this effect, it is proposed to impose restrictions on the motion of the tether about the pitch axis, which formally reduces the number of system degrees of freedom. This allows the implementation of the set motion mode with control only on the remained degree of freedom. The type of such restrictions is defined based on physical reasons. By accounting for all requirements for the mode of additional deployment, it is possible to develop the law of varying the pitch angle over time, which is described by a seventh-order polynomial. Detailed numerical research on the effect of mode parameters, such as the duration of deployment and expected shape of the pitch angle law vs. time, on the length of the unrolled tether and the character of its behavior during deployment is conducted. An example is provided numerically for the application of the developed method. Numerical simulation of the mode is carried out within the integration of the initial value problem for the Hill-Clohessy-Wiltshire equations. Quantitative estimation of errors of numerical simulation is conducted. The results of the calculations are illustrated graphically.

Keywords*: space tether, deployment, control, length variation, vertical position, underactuated system.*

Цитування: Wang C., Zakrzhevskii A. E. Programmed control of additional deployment of a space tether with recovery of its initial vertical orientation. *Space Science and Technology.* 2024. **30**, No. 5 (150). P. 3—18. https://doi.org/10.15407/knit2024.05.003

1. INTRODUCTION

Various modes of the motion of space tethers are widely described in the scientific literature. Comprehensive analysis of potential applications for space tethered systems (STS) is carried out in publications [1, 4, 6, 13, 18, 20, 36]. The greatest number of publications in the field of STS dynamics are devoted to the modes of deployment and retrieval of these systems. The authors use different mechanical models of tethers. The detailed analysis of such models is given in [4, 13, 19, 31].

Many new methods have been developed for the creation of control for deployment and retrieval modes of space tethers in recent years. In [9], there is an in-depth examination of the control techniques and tactics employed by STS. A novel full-order sliding mode tension control scheme for the deployment/retrieval of the STS is proposed in [17]. The designed control technologies can guarantee the asymptotic stability of the full-order sliding mode dynamics. This method not only allows the system to adapt to uncertainty factors but also to bring it to a steady state within a limited time. A new fractional order tension control law is proposed in [27, 28] for stable tether deployment and retrieval. Unlike existing integer-order control laws, which are based on the feedback of the current state and memoryless, the fractional order control law has the memory of previous states and thus controls the tether retrieval more smoothly while maintaining the retrieving speed.

An adaptive super-twisting control for the deployment of space-tethered systems with the consideration of uncertainty of external and internal disturbances with unknown boundaries is proposed in [10]. Control of deploying to a predetermined length of an extended tether system into the vertical position is considered in [32]. The STS model has distributed parameters, in which the thread is represented as a set of point masses connected by elastic links.

Widespread attention to the dynamics of space formation has led to increased research in this area in recent years. The main reasons for the growing interest in the study of tethered formation lie in its promised applications in space, such as interferometric measurements, cargo transportation, auroral observation, and stereoscopic observation. The spinning stability of a triangular tethered satellite formation that flies in low Earth orbit is studied in [36]. A dynamic similarity between the on-orbit dynamics and ground experimental models is built to construct an equivalent ground experiment to verify the stability analysis. The dynamics and control of tethered satellite formations in low Earth orbits are studied in [7]. Analysis of the deployment of a three-mass tethered satellite formation is presented in [8]. The orbital tethered system consists of three nanosatellites connected via tethers end-to-end, and the desired arrangement for the end masses is an equilateral triangle. Dynamic behavior analysis and stability control of tethered satellite formation deployment are studied in [38]. Two stability control laws for tether release rate and tether tension are proposed here to control tether length variation. A sliding mode adaptive control strategy of a spinning electrodynamic tether formation during its spin-up process is proposed in [14, 15] to track spinning motion and stabilize deformation by adjusting only electrical current.

Interest in the problem of space debris, which has increased in recent years, has initiated the emergence of research connected with the use of STS for removing spacecraft from orbits after they have finished functioning. For example, [24] studies the deployment dynamics of proposed novel tether configurations for orbital debris removal. Tether elements are simulated using two numerical models: a lumped mass node system connected by massless spring-damper elements and an absolute nodal coordinate formulation model. The paper [21] provides novel insights into the feasibility of tether de-orbiting for various mission phases, such as stabilization after capture, de-orbit burn (plus stabilization), and stabilization during atmospheric pass, highlighting the importance of various critical mission parameters, such as the tether material.

Many approaches to the deployment of tethers in the position along the local vertical are known. It is connected with the fact that the vertical configuration of a tether of constant length is steady relative to the local vertical [16]. Such a deployment is carried out, as a rule, during two stages. Free deployment is used in most cases at the initial stage. [26]. The system of deployment gives an initial impulse to a subsatellite, and the thread is unwound without resistance. At the end of the first stage, the thread is

broken, and after its tension, the tether enters the mode of libratory oscillations under the influence of the restoring torque of the gravity forces. A long time is required to stop the tether in a radially aligned position. This time will be spent on internal damping in the viscoelastic thread. Yet there are methods of acceleration of this mode. Such a case is studied in [2]. The pendular oscillations, which arise during the primary deployment of the tether with the viscoelastic thread, are damped parametrically. In this mode, the thread is pulled in at the return points of librational oscillations and is released near the local vertical periodically. Such a mode is directly contrary to the parametrical excitation of pendulum oscillations.

Reference [3] is devoted to the study of tension control of a tether at the first stage of deployment. The various ways of tether deployment with speed control are described and analyzed in [4, 12, 13, 19]. One can assign to shortcomings of such a control method the fact that it is difficult to damp longitudinal elastic oscillations of a tetherat its use. Considerable longitudinal oscillations can cause the tether to lose the tension of the thread. It, in turn, will lead to the loss of control of its deployment/ retrieval.

Tether tension control is widely described in the literature. This control gives an opportunity for damping of elastic longitudinal oscillations of the tether if they occur. The various strategies for control in such deployment scenarios and devices for their implementation are discussed in [5, 8, 15, 17, 23, 27, 28—30, 33, 34, 39]. The problem of optimal control for high-speed performance is solved for a simple system with a massless thread in [25]. The law of relay control of the thread tension is determined as a result. The advantage of this method is that it allows deploying a tether from one vertical position in the same another at minimum pitch angles. The shortcomings of such control are that implementation of the relay law is rather difficult, especially with the weak thread tension. Besides, the possibility of initiation of longitudinal elastic oscillations at relay control is very high.

From a practical point of view, there is no need to hold the tether in close proximity to the local vertical during deployment. It is enough that the control should lead the tether to the local vertical at the end of the process.

Many mechanical models of space tethers with massless thread are known, the motion of which occurs in a circular orbit. Only one control channel related to the change in tether length is used in such models (tether length control. deployment speed control, and tension control). At the same time, the number of degrees of freedom in this mechanical model equals two. The second degree of freedom is connected with the motion of a tether about the pitch axis. Such a tether can be considered as an underactuated mechanical system in which the number of degrees of freedom is greater than the number of control channels. This feature of the mechanical model of a tether with massless threads was ignored for a long time. As a result, for example, the problem of deployment of the tether in a vertical position had no practical solution for a long time.

Recently, interest in such underactuated mechanical systems has increased. In [39], the tether is considered as an underactuated mechanical system. A new controller for the modes of tether deployment and retrieval based on the use of a formed virtual signal is offered there. The authors showed that the pitch angle, which has no direct control, can be operated using data on tether length. Considering the underactuation problem of the electrodynamical tether, a sliding mode controller with an adaptive law is proposed to track spinning motion and stabilize deformation by adjusting only electrical current [14,15]. The discussion of the deployment strategy for a 3-body chain-type tethered satellite system in a low-eccentric elliptical orbit is presented in [11]. Two deployment strategies are discussed. Then, the tension on the tether is used to deploy it to the desired length and suppress its sway motion, resulting in an underactuated and input-constrained system. Hierarchical sliding mode control with anti-windup technology is employed to overcome the above challenges. The study of the underactuated attitude tracking control problem of a tethered spacecraft during tether deploying and spinning is presented in [30]. The main contribution here is the development of an underactuated tracking controller with an adaptive barrier function that inhibits unknown disturbance. A sliding mode control approach is proposed to stabilize a class of underactuated systems that are in cascaded form [35].

The difficulties in implementing the scenarios described above and the difficulties of creating control laws for the modes of tether deployment/retrieval in the steady vertical configuration in orbit can be avoided by imposing additional constraints on the system to reduce the number of its degrees of freedom. This will make the system no longer underactuated, and the problem of developing the programmed control for the considering mode of deployment becomes significantly simplified. The restrictions should align with the parameters of the mode being studied, focusing on determining suitable pitch angle behavior over time. Further details on how to achieve this, based on the work [37], will be provided.

2. MATHEMATICAL MODEL OF THE SYSTEM

Choose two equal point masses connected by an elastic massless thread as the mechanical model of the tether. As we do not consider the modes of the tether motion when the thread can be reeled up on the end bodies, the geometrical sizes of the end bodies do not matter. The assumption of massless thread is justified for tethers with light threads made of modern synthetic materials. The analysis, which was performed in [23], showed that accounting of the mass of thread in the model of the tether does not result in essential differences in the motion of such a tether from the motion of a tether whose mass is concentrated in the end bodies.

As shown in calculations, the distance between the mass center of the tether of considered types and its center of gravity is significantly less than the length of the tether. Therefore, we will consider that the tether mass center moves on an orbit.

Introduce an orbital reference system $Cx^{or}y^{or}z^{or}$ with the origin at the tether mass center. Let the axis Cx^{or} be directed along the geocentric position vector, Cy^{or} along the orbital velocity, and Cz^{or} along the normal to the orbit plane. Thus, the axes Cx^{or} and Cy^{or} lie within the orbit plane, while the axis Cz^{or} lies outside it.

Choose the central Newtonian force field as the gravitational field model. Determine the position vectors $\mathbf{r}_1, \mathbf{r}_2$ of point masses in relation to the point C by their projections in the orbital frame of reference:

$$\mathbf{r}_1 = \{ x_1^{or},\ y_1^{or},\ z_1^{or} \},\ \mathbf{r}_2 = \{ x_2^{or},\ y_2^{or},\ z_2^{or} \}.$$

Choose these projections and their time derivatives as phase variables of the problem.

3. TETHER LENGTH EXTENSION SCENARIO

For a demonstration of opportunities of the proposed method, consider further the problem of the length extension of two bodies tether with massless connection, which is already deployed, aligned to the local vertical, and its length is L_0. Let us demand that the tether should be aligned to the local vertical again after the increase in length up to the set value L_F. Now it is necessary to obtain the expression for the constraint imposed on the uncontrollable variable which is the pitch angle ϑ. Consider the tether distance between bodies' mass centers as a control variable. Upon an increase in length, according to the theorem of change of angular momentum, the tether begins to deviate towards negative values ϑ since its angular momentum does not change considerably at a small pitch angle when the gravitational torque is small. Since the tether should be motionless on the local vertical at the initial and final instants by the terms of the problem, the following conditions should be satisfied:

$$\vartheta(0) = 0, \quad \vartheta(T_F) = 0, \tag{1}$$

$$\dot{\vartheta}(0) = 0, \quad \dot{\vartheta}(T_F) = 0. \tag{2}$$

Here, T_F is the time of termination of the deployment mode, the dots over the variables indicate their differentiation with respect to time t.

As a result, the dependence $\vartheta(t)$ as a rough approximation may look as in Figure 1. In the beginning, the tether deviates in the negative direction about the axis Cz^{or}, thereby causing the emergence of the gravitational torque, which counteracts this deviation. At rather large deviations, the gravitational torque aims to recover the vertical orientation of the tether. The research objective is to construct such a law of change of the tether length, in which the gravitational torque, increasing the angular momentum of the tether, leads it to the local vertical with the performance of conditions (2).

Conditions (1) and (2) do not reflect all of the requirements of practice imposed on the tether within the considered deployment mode. The following conditions should be satisfied during the tether deployment, from initial length L_0 to final length L_F:

$$L(0) = L_0\,, \quad L(T_F) = L_F\,. \tag{3}$$

The first of these conditions is met in advance, the second condition can be used later to determine the time T_F unknown in advance. This value will allow choosing the suitable solution to the problem from the set of solutions obtained for various values T_F or other parameters of the deployment process that have an influence on the final length of the tether.

Two more conditions follow from the requirement of constancy of the tether length at the initial and final instants:

$$\dot{L}(0) = 0\,, \quad \dot{L}(T_F) = 0\,. \tag{4}$$

The emergence of jumps of tension in the thread is inadmissible, both at the initial and final instants of the process and during all maneuvers, as they can lead to the disappearance of thread tension. It will make the accepted mechanical model inadequate. The lack of jumps in tension at the initial and final instants is reached when the following conditions are met:

$$\ddot{L}(0) = 0\,, \quad \ddot{L}(T_F) = 0\,.$$

These conditions follow directly from the tether equation of longitudinal motion in spherical coordinates [4] (the case of motion in the orbit plane), which, with the notations accepted here, takes the form

$$\ddot{L} = L[(\dot{\vartheta} + \omega^{or})^2 + 3(\omega^{or})^2 \cos^2\vartheta - (\omega^{or})^2] - 2T/\bar{m}\,. \tag{5}$$

Here ω^{or} is the orbital angular speed, T is the tether tension force, $\bar{m} = m_1 m_2/(m_1 + m_2)$, m_1, m_2 are the end bodies masses.

Really, when performing conditions (1), (2),

$$\ddot{L} = L3(\omega^{or})^2 - 2T/\bar{m} = 0. \tag{6}$$

Now, it is necessary to construct the tether length control law that allows us to achieve our objective of deploying the tether "from rest to rest" to the set length. The physical interpretation of this control is as follows: the angular momentum of the tether changes during deployment under the influence of the gravitational torque to a vector value that corresponds to the angular momentum of the vertically aligned tether at $t = T_F$.

Use the motion equation of an inextensible tether of variable length in spherical coordinates for in-plane rotation to create the necessary program control law. Following [4], it is possible to provide the tether motion equation in the orbit plane in the following form:

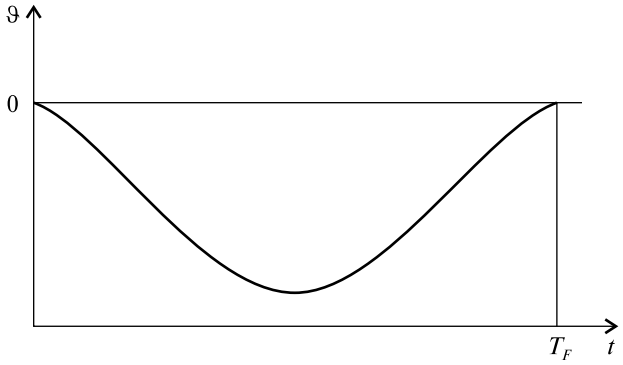

Figure 1. A rough approximation of the dependence $\vartheta(t)$ during deployment

$$\ddot{\vartheta} + 2(\dot{\vartheta} + \omega^{or})\dot{L}/L + 3(\omega^{or})^2 \sin\vartheta\cos\vartheta = 0\,. \tag{7}$$

From this equation, one can obtain the ordinary differential equation of the first order with the corresponding initial condition

$$\dot{L} = -L\frac{3(\omega^{or})^2 \sin 2\vartheta + 2\ddot{\vartheta}}{4(\omega^{or} + \dot{\vartheta})}\,, \quad L(0) = L_0\,. \tag{8}$$

Assuming that the law of change is known, the solution of equation (6) can be expressed as follows

$$L(t) = L_0 \exp\left[-\int_0^t \frac{3(\omega^{or})^2 \sin 2\vartheta(\tau) + 2\ddot{\vartheta}(\tau)}{4(\omega^{or} + \dot{\vartheta}(\tau))} d\tau\right]. \tag{9}$$

Taking into account condition (8) and equation (4), it is possible to obtain two more conditions for the pitch angle:

$$\ddot{\vartheta}(0) = 0\,, \quad \ddot{\vartheta}(T_F) = 0\,. \tag{10}$$

Returning to Figure 1, one may see that to give the law of change $\vartheta(t)$ a form close to that shown in the Figure, it is sufficient to define at least one point on this curve. It should be noted that the problem of choosing such a point is ambiguous. Let us choose, for example, the point $t = T_F/2$ and set the following condition:

$$\vartheta(T_F/2) = F_{sr}\,.$$

Here, F_{sr} is the unknown, in advance, amount of the tether deflection on the pitch angle, which can be chosen later during numerical simulation as a problem parameter. It is possible to introduce additional parameters of the law $\vartheta(t)$ shape here. For example,

as such a parameter, one may introduce the relative instant $\tau = aT_F T_F$ that allows writing down

$$\vartheta(t) = F_{sr}. \qquad (11)$$

Using already found restrictions for $\vartheta(t)$, after differentiation equation (8) with respect to time, it is possible to obtain the following restrictions from conditions (5):

$$\ddot{\vartheta}(T_0) = 0, \quad \ddot{\vartheta}(T_F) = 0. \qquad (12)$$

Thus, for the creation of the program law of change J(t), one can use nine conditions (1), (2), (10)—(12).

Setting various values of the duration T_F, one can obtain the various dependencies of the tether length $L(t)$. Then, from this set of solutions, one law can be selected that corresponds to the given final length of the tether, does not lead to a loss of tension in the thread during deployment, and meets the other described requirements.

One can construct the necessary law $\vartheta(t)$ as any finite power series. Its coefficients can be found from the above-mentioned nine conditions. For example, let the law $\vartheta(t)$ be in the form of a power series of the eighth order

$$\vartheta(t) = \sum_{i=0}^{7} c_i \left(\frac{t}{T_F}\right)^i. \qquad (13)$$

Its coefficients found from nine conditions (1), (2), (10)—(12) have the following expressions:

$$\begin{gathered} c_0 = 0,\ c_1 = 0,\ c_2 = 0,\ c_3 = 0, \\ c_4 = F_{sr} / ((-1 + aT_F)^4 aT_F^4 T_F^4), \\ c_5 = -4 \cdot F_{sr} / ((-1 + aT_F)^4 aT_F^4 T_F^5), \\ c_6 = 6 \cdot F_{sr} / ((-1 + aT_F)^4 aT_F^4 T_F^6), \\ c_7 = -4 \cdot F_{sr} / ((-1 + aT_F)^4 aT_F^4 T_F^7), \\ c_8 = F_{sr} / ((-1 + aT_F)^4 aT_F^4 T_F^8). \end{gathered} \qquad (14)$$

The law $L(t)$ obtained according to expression (13) depends on the law $\vartheta(t)$, which, in turn, depends on the duration of the deployment mode, parameters F_{sr}, aT_F, and orbit radius, which defines the gravitational torque value.

4. NUMERICAL INVESTIGATION OF APPROPRIATE CONTROL LAW

Further, consider the implementation of the offered method for creating the programmed control. Without breaking the generality of the problem statement, simplify the description by considering a tether with two identical end bodies. Initially, the tether was deployed and aligned to the local vertical. It also should remain along the local vertical at the end of deployment. At the same time, the tether should have a set length $L(T_F) = L_F$.

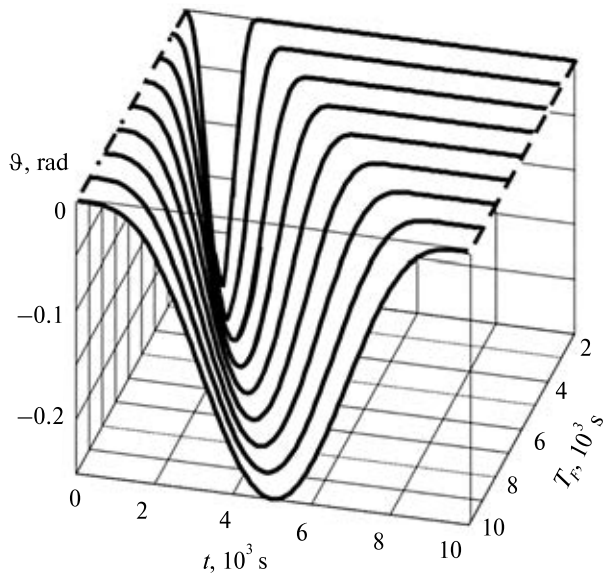

Figure 2. Behavior of the pitch angle $\vartheta(t)$ vs. time t at different values of the deployment duration T_F

Table 1. **Parameters of Case 1**

Parameters	Variants			
	1_1	1_2	1_3	1_4
F_{sr}, rad	−0.1	−0.15	−0.20	−0.25
aT_F	0.2	0.3	0.4	0.5

Choose the following values for the tether parameters:

- The end bodies have masses of 10 kg.
- The initial length of the tether is 3000 m.
- The orbit radius is 7000 km.

Let us proceed to find the law $L(t)$ that solves the problem.

Initially, consider several various values of the parameters F_{sr} and aT_F for various values of the deployment duration in the range of T_F=1000...10000 s. (Case 1). Values for parameters F_{sr} and aT_F are given in the Table 1.

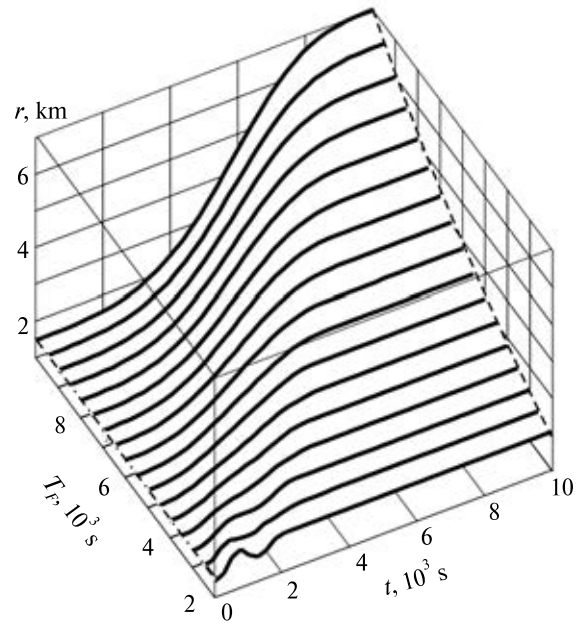

Figure 3. Laws of change of the top branch length r vs. time at different values of the deployment duration T_F

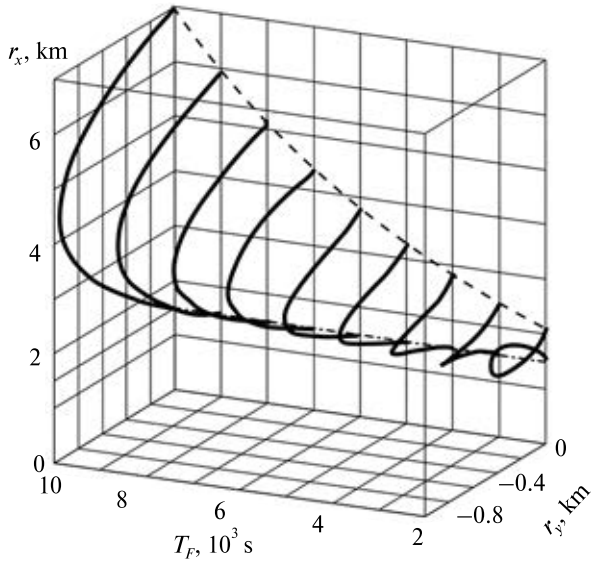

Figure 4. The trajectories of the higher-end body vs. deployment duration T_F

In Figure 2, curves $\vartheta(t)$ are displayed for variant 1_4 at different values of the deployment duration T_F in the accepted range according to formula (13). Each line in this plot corresponds to a duration of the specific mode. The dot-dash line in Figure 2 and all other Figures represents the initial condition of the end body of the top branch. The dashed line represents its final position. In the plot, it is evident that as the value T_F changes, the shape of the curve $\vartheta(t)$ changes slightly, stretching along the time axis. To evaluate the acceptability of any given program law of motion, it is crucial to construct the programmed law of change of the tether length $L(t)$ over time.

Solving the initial value problem (8), one can obtain this law for the number of values T_F at the known laws $\vartheta(t)$. The obtained law can only be implemented if the tension force of the tether does not take negative values. Attempts to construct such laws for the variants of the parameters given in Table 1 showed that for variant 1_1, the negative values of the tension force disappear only for values $T_F \geq 3000$ sec. For other variants from Table 1, the maximum value T_F, at which the tension of the tether takes negative values at certain time intervals, falls to 2000 sec. It is simple to clarify this fact. With this initial length of the tether and mass of the end body, the speed of increase in the length of the tether is insignificant. Therefore, the tether cannot significantly extend in a short period and considerably deviate towards negative values of the pitch angle. So, in such cases, the essential gravitational torque, which may turn it to the local vertical at the end of the mode, is absent.

Since the shapes of the constructed curves for the considered deployment modes for variants 1_1...1_4 differ qualitatively insignificantly, plots of the main values only for variant 1_3 are provided further. In Figure 3, laws of change in the top branch length versus time are shown at values T_F ranging from 2000 sec to 10000 sec. As seen in this Figure, the law of change of length r_1 is not monotonous for the values of T_F at the initial part of the considered interval at the beginning of deployment. Here, one can see a change in the sign of the deployment speed, i.e., retraction of the thread. If the deployment system is not adapted for such a mode, then the found control laws can be realized only if $T_F \geq 4000$ sec. The final length of the tether increases not linearly with the deployment duration. This is natural because, with increasing the length of the tether, the force of its tension and the deployment speed increase. The graph shows that with increasing deployment duration, the law of change r_1 becomes smoother.

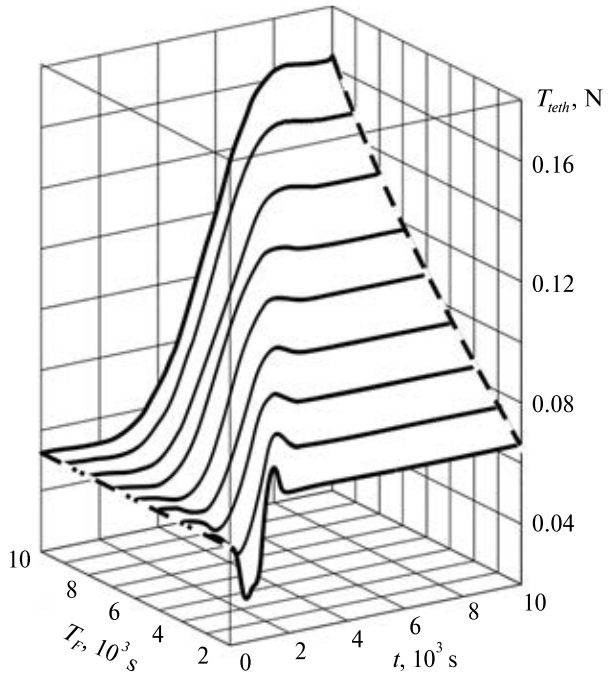

Figure 5. The thread tension vs. time t at different values of the deployment duration T_F

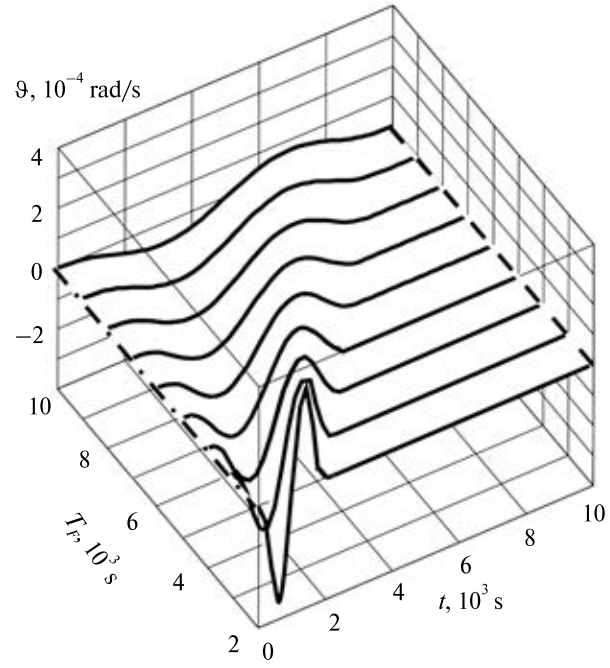

Figure 6. The tether angular speed $\dot{\vartheta}$ vs. time t at different values of the deployment duration T_F

In Figure 4, the trajectories of the higher-end body are shown in the orbital frame of reference at the same values of parameters F_{sr} and aT_F. Here, it is seen that the first two trajectories on the right have the shape of loops. This explains the occurrence of time intervals in Figure 3, where the length r_1 is reduced during deployment. Note that the scales of deviation of the end body along axes Cx^{or} and Cy^{or} do not coincide in Figure 4. This is done in order to better describe the shape of trajectories in detail.

In Figure 5, laws of change of the thread tension are shown. Here, one can see that the tension force decreases at the beginning of deployment as a result of the thread unwinding. The shorter the deployment duration, the more pronounced this effect becomes. This effect is expressed especially strongly for the deployment with $T_F = 2000$ sec. The tension force begins to decrease slowly at the end of deployment when the tether approaches the local vertical. Then, it slightly decreases when the tether reaches the local vertical after the damping of inertial forces and becomes equal to the steady-state value of the tension for a tether located along the local vertical according to the formula (6). However, there are no time intervals during which the tension force takes negative values in the case being considered.

Figure 6 depicts the change of the tether's angular speed $\dot{\vartheta}$ versus time in its angular displacement about the pitch axis for the range of $T_F \in [2000,10000]$ sec. This angular speed in the considered deployment mode always takes negative values. Besides, the modulus of the angular speed of the tether $\dot{\vartheta}$ in the orbital frame cannot be more than the orbital angular speed ω^{or} in this mode in the time interval $t \in [t_0, T_F]$. Otherwise, when approaching zero value at the end of the deployment, it will take the negative value the module of which is equal to the value of the orbital angular speed. In such a case, the denominator in the right part of equation (8) will turn into zero, and the equation (8), from which the control law can be found, will degenerate. In terms of mechanics, such a case corresponds to the tether translator motion in the inertial frame of reference.

Figure 7 presents graphs of the program laws of the deployment speed (change of the vector $\mathbf{r}_1$ length) versus time at the same values of the parameters F_{sr} and aT_F. Here, one can see that negative speed val-

ues disappear only on the third curve on the right, for which $T_F = 4000$ sec. As the deployment duration increases, the curves become smoother.

Further, the following options of the parameters were considered (Case 2, see Table 2).

The power series (13), as it is demonstrated by the formulas (14), exhibits point symmetry of the dimensionless parameter aT_F with respect to $aT_F = 0.5$. For physical reasons, this parameter's value cannot be in any way near zero or one. With such values aT_F, the coefficients in the series (13) are equal to zero, and the problem statement becomes meaningless. One can see that in Fig. 8. The further the value aT_F deviates from 0.5, the greater the tether length at the end of deployment. Observe that the maximum deviation of the tether on the pitch angle is also increasing simultaneously. This value seems to be greater than the F_{sr} value that is fixed at the point $\tau = aT_F T_F$.

In Figure 8, the dashed line shows the dependence of the final length of the tether branch on the parameter aT_F for variant 2_1. This 3D plot, as well as the plot shown in Fig. 9, has mirror symmetry with respect to the plane $aT_F = 0.5$.

Figure 9 also shows trajectories of the end body by variant 2_1 (Table 2). With such parameters, all trajectories turn out rather smooth. The control laws constructed for the considered values of parameters allow increasing the length of the top branch of the tether from one and a half km to seven km.

The influence of the parameter F_{sr} on the control law character was studied further (Case 3). The variants given in Table 3 were considered.

An increase in the tether length with the parameter values following from variant 3_3 has a smooth character (Figure 10, *a*), although, for variants 3_1, 3_2, this character changes slightly (Figure 10, *b*). Additionally, comparing Figure 10, we can conclude that if the deployment duration T_F is doubled at the same values of

Table 2. **Parameters of Case 2**

Parameters	Variants		
	2_1	2_2	2_3
F_{sr}, rad	–0.15	–0.25	–0.50
aT_F	0.3...0.75	0.3...0.75	0.3...0.75
T_F, sec	5 000	10 000	10 000

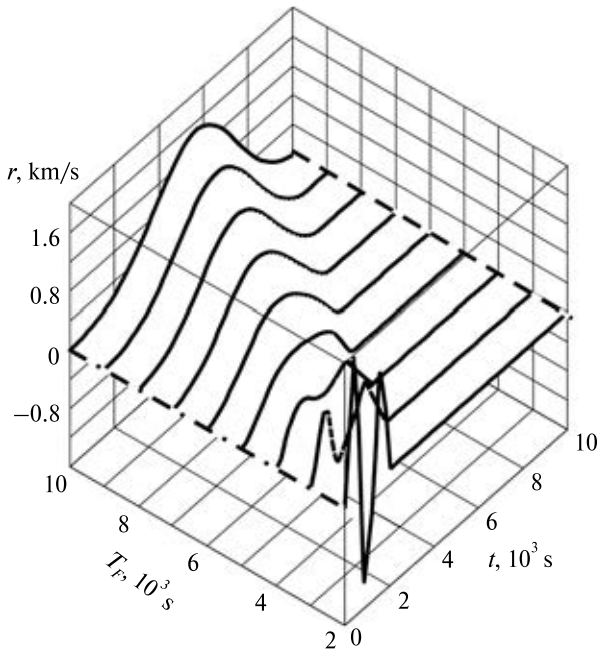

Figure 7. The deployment speed $\dot{r}_1$ vs. time t at different values of the deployment duration T_F

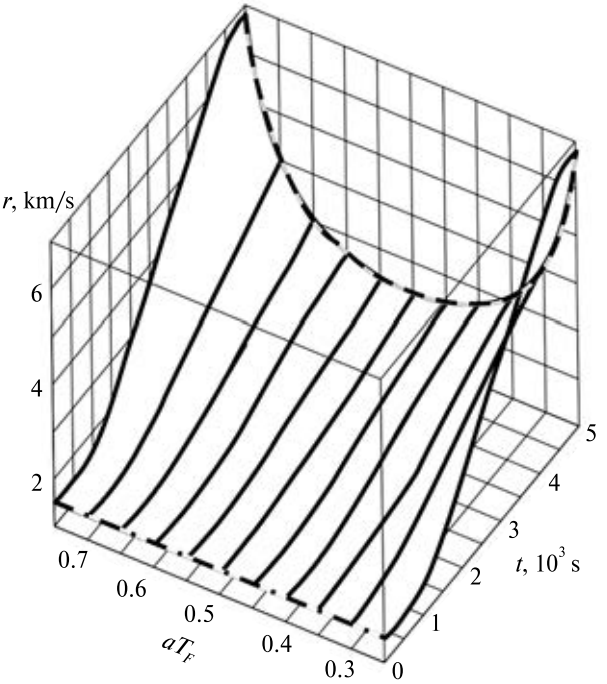

Figure 8. Laws of change of the top branch length r vs. time t at different values of the parameter aT_F

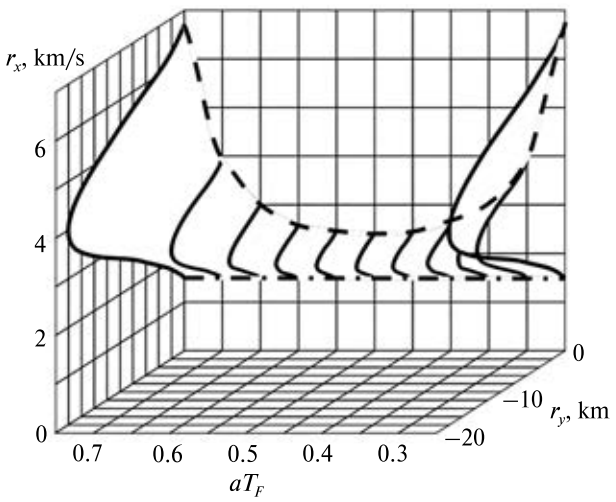

Figure 9. The trajectories of the higher end body at different values of the parameter aT_F

Table 3. **Parameters of Case 3**

Parameters	Variants		
	3_1	3_2	3_3
F_{sr}, rad	−0.1...1.0	−0.1...1.0	−0.1...1.0
aT_F	0.5	0.5	0.5
T_F, sec	3000	5 000	10 000

parameters F_{sr} and aT_F, then the final length of the tether increases approximately four times.

The maximum length of deployment significantly depends on the value of the parameter F_{sr}, which determines the maximum deviation of the tether by the pitch angle. If, at $F_{sr} = -0.1$ rad, the 1.5 km long tether branch can be increased by only hundreds of meters in 10000 sec, then, at $F_{sr} = -1$, this length can be increased to dozens of kilometers. The research on the tether tension force for the considered parameters showed that for the cases corresponding to values $F_{sr} = -1$ rad and $F_{sr} = -0.9$ rad, there are time intervals between $t = 1000$ sec and $t = 2000$ sec where the tension force takes negative values. This area is outlined with a medium-thickness line in Figure 11 from the left. Naturally, such modes of deployment cannot be realized. This situation is explained by the fact that in the mechanical system under consideration, with the deployment duration of 5000 sec, it is

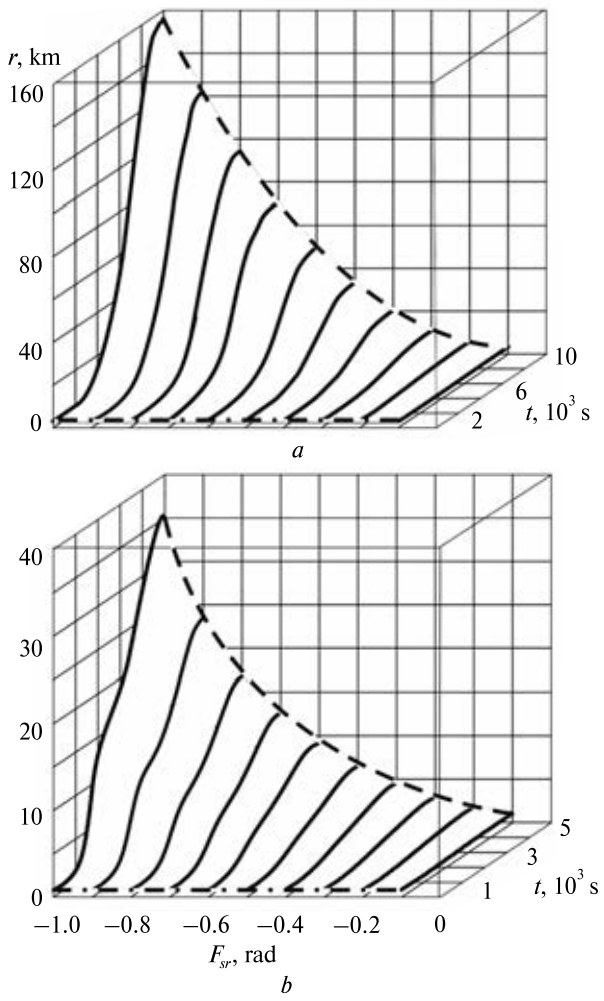

Figure 10. Laws of change of the top branch length r vs. time t at different values of the parameter F_{sr} and deployment duration: a — T_F=10000 s, b — T_F=5000 s

not possible to reach such an angular deviation only due to the Coriolis force.

Figure 12 plots the velocity of the thread exit versus time. One can see here that the velocity of the thread exit is required to be very high in this time interval for cases $F_{sr} = -1$ rad and $F_{sr} = -0.9$ rad. In this case, such speeds cannot be reached by tether tension only. Therefore, there is an area of negative values of the tension of the tether, shown in Figure 11.

Trajectories of the tether's higher end body in projection on the plane $Cx^{or}y^{or}$ of the orbital frame are shown in Figure 13. Here, as well as in Figure 9,

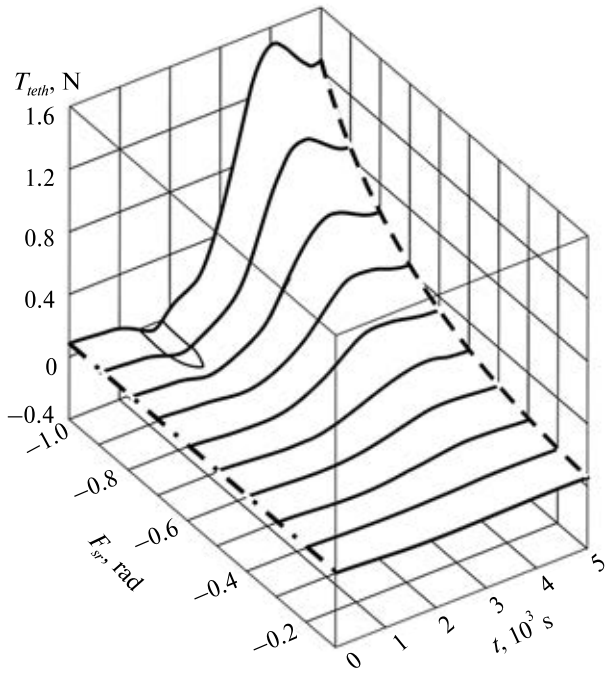

Figure 11. The tether tension force T vs. time t at different values of the parameter F_{sr} and deployment duration $T_F = 5000$ s

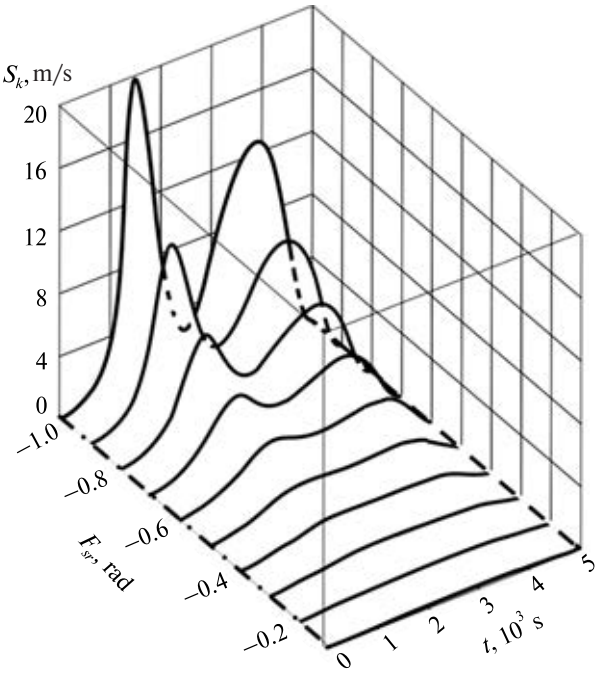

Figure 12. The velocity of the thread exit vs. time t at different values of the parameter F_{sr} and deployment duration $T_F = 5000$ s

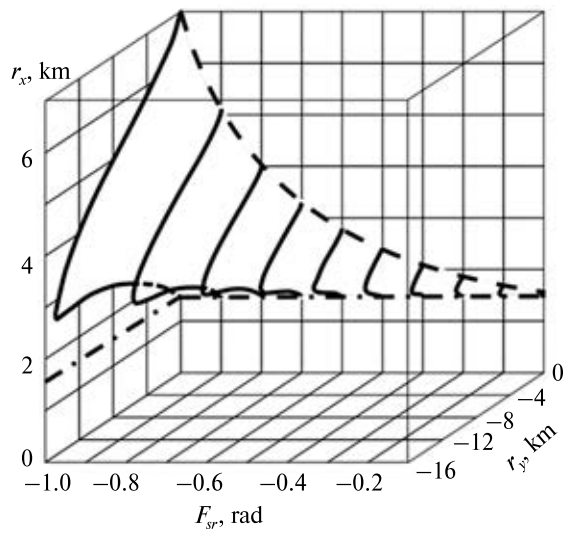

Figure 13. The trajectories of the higher end body at different values of the parameter F_{sr}

scales on the Cx^{or} and Cy^{or} axes are chosen differently to show the trajectories' shapes better. The shape of the trajectories of the end body becomes smoother and smoother as the absolute value of the parameter F_{sr} decreases. Judging by these plots, loops may appear on the trajectories when F_{sr} is further increased in absolute value. At the same time, deployment will become more technically challenging. If the deployment duration is increased from 5000 up to 10000 sec, trajectories will have such a smooth character as the left trajectory in Figure 4.

5. NUMERICAL SIMULATION OF PROGRAMMED-CONTROLLED DEPLOYMENT

Let us apply the obtained results to create the control law for the deployment of the tether aligned along the local vertical to the pre-specified length with the preservation of the final vertical orientation. Consider the tether of two point masses of 10 kg each, with an initial length of 3000 m. Investigate the process of its deployment to a length of 60,000 m. If the parameters of the mode are set to $F_{sr} = -0.5$ rad and $aT_F = 0.5$, then it is only necessary to define the adequate deployment duration T_F. Using the results of the previous numerical research, we establish by interpolation that the required deployment duration with an accuracy of up to 1 second is equal to 9939

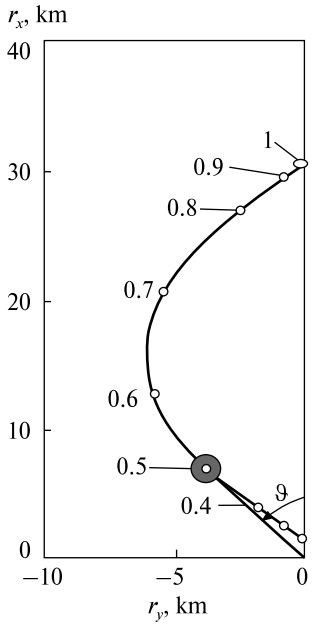

Figure 14. The trajectory of the higher end body as a result of the simulation of the deployment process (numbers near the curve — the value of t/T_F)

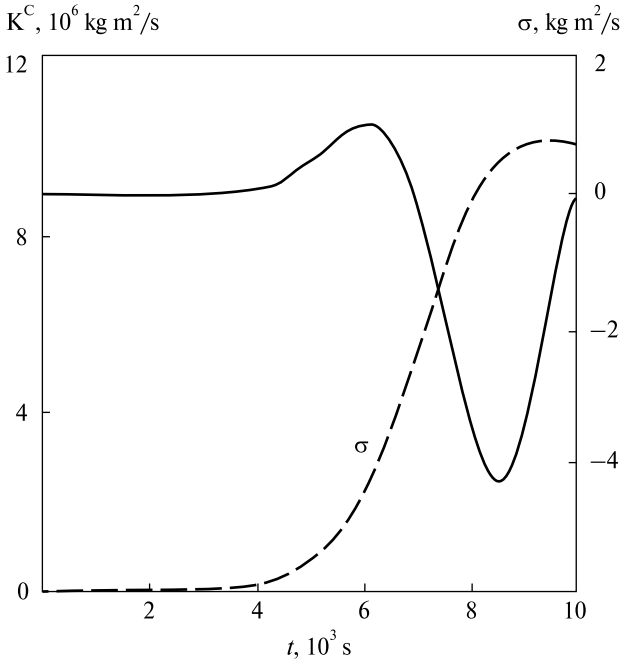

Figure 15. The magnitudes of the angular momentum vector $\mathbf{K}^C$ and errors σ of simulation vs. time t

seconds. With such deployment duration, the tether length has to become equal to 60001.7 m. If necessary, the accuracy of the calculation can be slightly increased. This can be done by correcting both the T_F values and other parameters. Now, it is necessary to carry out the numerical simulation of the deployment process controlled by the found program law.

For this purpose, use motion equations of the tether of variable length in the form of the equations of Hill-Clohessy-Wiltshire (HCW), which describe the space motion of point masses concerning the mass center of the tether [9]. Following the traditional derivation of these equations, with the chosen direction of axes of the orbital reference frame, they can be written in the following vector form:

$$\ddot{r}_i = \{2\omega^{or}\dot{y}_i^{or} + 3(\omega^{or})^2 x_i^{or} - Te_{ri}(1)/m_i - $$
$$-2\omega^{or}\dot{x}_i^{or} - Te_{ri}(2)/m_i - $$
$$-(\omega^{or})^2 z_i^{or} - Te_{ri}(3)/m_i\}, \ (i = 1, 2). \qquad (15)$$

As length is not included obviously in the equations, knowing program laws of change in time of the pitch angle and length of the tether, based on equation (5), one can construct the programmed law of change of the tension force. Consequently, the equations (15) will be completed, and one can carry out a numerical simulation of the tether deployment.

The trajectory of the end body motion of the top tether branch is plotted on the plane $Cx^{or}y^{or}$ as a result of the numerical solving of the initial value problem for HCW equations (15) with the accepted initial conditions. This trajectory is shown in Figure 14. The scale of deviations of the end body along both axes of the orbital reference frame is not equal in this plot. Points with a notation of the relative time instant corresponding to each of them are plotted on the trajectory. The top branch of the tether is depicted at the instant $t = T_F/2$. One can see from the plot how uneven the motion of the end body along the trajectory is. Such irregularity is formed as a result of the dependence of the speed of the tether deployment on its tension and, consequently, on its length. Therefore, the finishing part of the trajectory is completed much quicker than its initial part having the same length. The tether branch length is increased from the initial value of 1500 m to 30000.85 m during 9939 sec as a result of applying the constructed program control.

Numerical integration of the initial value problem was carried out by Runge-Kutta's method with the constant integration step of 0.01 sec.

To take the elasticity of the thread into account, a correction should be entered into the computing program for the calculation of the real distance between end-bodies. The length of the deployed stretched thread should be controlled during deployment according to the solution (9), i.e., $L = L(t)$. This means that if the deployment device fixes the length of the non-stretched thread $\bar{L}(t)$, then the correction $\bar{L}(t) = L(t) - \Delta\bar{L}(t)$ should be entered into the control law for the real deployment system. Here, $\Delta\bar{L}(t) = T(t)L(t)/(EF + T(t))$, EF is the thread extensional stiffness. It is rather simple to implement such an adjustment by measuring the tension or using its program values. If the current distance between the tether bodies is measured during deployment, then there is no need to make corrections for the law of change of the tether length.

The monitoring of the errors of calculations was carried out during numerical simulation. The current magnitude value of the angular momentum vector, constructed based on the current values of the phase variables of the problem for the equations (15), was compared to its values obtained from the theorem of change of the angular momentum of the tether under the gravitational torque effect. In Figure 15, the continuous line corresponds to the magnitude of the angular momentum vector of the tether. For both calculation cases, these curves on graphics practically coincide. The dashed line characterizes the difference in the calculation of these values in two specified ways. It is obvious that errors in calculations are quite acceptable for the practice.

6. CONCLUSIONS

Summing up the results, one can say that a new method of program control by the additional deployment of a space tether has been developed, which, in terms of the control theory, is an underactuated mechanical system. The tether model used in creating the programmed control law consists of two point masses connected by a massless elastic thread, moving in the plane of a circular orbit in the central Newtonian field of forces and described by ordinary differential equations in spherical coordinates. This mechanical model has two degrees of freedom and only one control channel. Considering that the tether moves in the gravitational field of forces, a new approach is proposed for the development of the control for underactuated systems. We have imposed restrictions on the tether pitch motion that allow controlling the pitch motion of the tether, using active control only by its length. Physical reasons were used to formulate the necessary constraints, and methods for solving the inverse problems of the dynamics were used for the creation of the control law based on the tether's length. As a result of the conducted research, the program control has been developed, which has allowed for solving the problem related to the mechanical model of the specific tether with three degrees of freedom.

Using such a control law, it is possible to deploy a tether from the initial state along the local vertical in the same vertical position, but already with a greater length, the size of which can be set in advance. We have conducted numerical research, which has allowed us to define the influence of various parameters of the control law on the behavior of a tether during deployment. Graphs have been plotted for various sets of parameters, which give an idea of the character and numerical characteristics of the dynamic processes when performing deployment. Since the created control law provides a quasistatic change of the tether parameters, accounting for the elastic properties of the thread is carried out in a quasistatic approach. The error estimation is carried out during the numerical simulation of the deployment of a specific tether to the specified length. This makes it possible to gauge the veracity of the data acquired and demonstrates the practical applicability of the strategy.

Acknowledgements. The authors thank Dr. Arun Banerjee, Former Principal Research Scientist, Lockheed Martin Advanced Technology Center, Palo Alto, CA, USA, for help with the technical writing of the manuscript.

Declaration of Competing Interest. The authors declare that they have no known competing financial interests or personal relationships that could have appeared to influence the work reported in this paper.

Formatting of funding sources. This research did not receive any specific grant from funding agencies in the public, commercial, or not-for-profit sectors.

Annex Nomenclature

aT_F	= parameter of control law shape
c_i ($i = 0, ..., 7$)	= coefficients of power series
EF	= thread longitudinal rigidity
$e_{ri}(j)$ ($i = 1, 2; j = 1, 2, 3$)	= directing cosines of position vectors of point masses in the orbital frame of reference
F_{sr}	= parameter of control law shape
$\mathbf{K}^{\mathrm{C}}(t)$	= vector of t angular momentum about mass center C
$K_3^{\mathrm{C}}(t)$	= projection of angular momentum on Cz^{or} axis
L, L_0, L_f	= current, initial, and final distance between end point masses
m_i ($i = 1, 2$)	= masses of end-bodies
$\mathbf{m}^{\mathrm{C}}(t)$	= vector of external torque
$M_g(t)$	= magnitude of gravitational torque
$\mathbf{r}_1$, $\mathbf{r}_2$	= position vectors of point masses relative to point C
$r(t)$	= magnitude of position vectors
$r_p(t)$	= programmed law of $r(t)$ change
$r_{pe}(t)$	= programmed law of $r(t)$ change with correction for elasticity
T	= force of thread tension
T_F	= duration of deployment
t	= time
$S(t)$	= speed of change of length $L(t)$
$x_i^{or}, y_i^{or}, z_i^{or}$ ($i = 1, 2$)	= projections of $\vec{\mathrm{r}}_1$, $\vec{\mathrm{r}}_2$ onto orbital frame
$\Delta r(t)$	= correction of program law $r_p(t)$ for the elasticity of thread
ϑ	= pitch angle
ω^{or}	= angular velocity of orbital tether motion

REFERENCES

1. Banerjee A. K., Kane T. R. (1982). Tether deployment dynamics. *Appl. Math. Comput.*, **30**, 347—366.
2. Barkow B. (2003). Controlled deployment of a tethered satellite system. *Proc. Appl. Math. Mech.*, **2**, 224—225. https://doi.org/10.1002/pamm.200310097
3. Barkow B., Steindl A., Troger H., Wiedermann G. (2003). Various methods of controlling the deployment of a tethered satellite. *J. Vib. Control.*, **9**, 187—208. https://doi.org/10.1177/1077546303009001747
4. Beletsky V. V., Levin E. M. (1993). *Dynamics of Space Tether Systems*. Univelt, San Diego.
5. Bindra Udai, Zhu Zheng H. (2016). Ground-based testing of space tether deployment using an air-bearing inclinable turntable. *Int. J. Space Sci. and Engineering*, **4**, No. 1, 1—17. https://doi.org/10.1504/IJSPACESE.2016.078571
6. Cantafio L. J., Chobotov V. A., Wolfe M. G. (1977). Photovoltaic gravitationally stabilized, solid-state satellite solar power station. *J. Energy*, **1**, 352—363. https://doi.org/ 10.2514/3.62346
7. Casas M. F. (2015). *Dynamics and Control of Tethered Satellite Formations in Low-Earth Orbits*. PhD Thesis Universitat Politecnica de Catalunya.
8. Chen S., Li Aijun, Wang Changqing (2020). Analysis of the deployment of a three-mass tethered satellite formation. *IOP Conf. Ser.: Mater. Sci. Eng.* 984 012028. https://doi.org/ 10.1088/1757-899X/984/1/012028
9. Clohessy W. H., Wiltshire R. S. (1960). Terminal guidance system for satellite rendezvous. *JGCD*, **27**, 653—658. https://doi.org/10.2514/8.8704
10. Dong Z., Zhang Lei, Li Aijun, Wang C., Shi Q. S. (2022). Adaptive super-twisting control for deployment of space-tethered system with unknown boundary disturbances. *Proc. IMechE. Part G: J. Aerospace Engineering,* **236**, No. 13, 2739—2750. https://doi.org/10.1177/09544100211068909
11. Jia C., Meng Z., Wang B. (2023). Deployment of three-body chain-type tethered satellites in low-eccentricity orbits using only tether. *Space Sci. and Technology*, **3**, No. 11, 1—9. https://doi.org/10.34133/space.0070
12. Levin E. M. (1983). On deployment of lengthy tether in orbit. *Kosmicheskie issledovanija*, **21**, 678—688.
13. Levin E. M. (2007). *Dynamic Analysis of Space Tether Missions*. Univelt, San Diego.

14. Lu H., Wang C., Li A., Guo Y. (2024). Sliding mode control strategy of spinning electrodynamic tether formation during its spin-up process. *IEEE Trans. Aerosp. Electron. Syst*., **60**, No. 1, 449—462. https://doi.org 10.1109/TAES.2023.3327700
15. Lu H., Yang H., Wang C., Li A. (2024). Nonlinear deformation and attitude control for spinning electrodynamic tether systems during spin-up stage. *Nonlinear Dyn.* (Early Access, https://doi.org/ 10.1007/s11071-024- 09415-z).
16. Lur'e A. (2002). A*nalytical Mechanics*. Springer. https://doi.org/doi: 10.1007/978-3-540-45677-3
17. Ma Zhiqiang, Sun Guanghui (2016). Full-order sliding mode control for deployment/retrieval of space tether system. *IEEE Int. Conf. on Systems, Man, and Cybernetics (SMC)*, 407—412, https://doi.org/10.1109/SMC.2016.7844275
18. Misra A. K. (2008). Dynamics and control of tethered satellite systems. *Acta Astronautica*, **63**, 1169—1177.
19. Modi V. J., Misra A. K. (1978). Deployment dynamics of tethered satellite systems. *AIAA Paper*, **1398**, 1—10. https://doi.org/10.2514/6.1978-1398
20. Padgett D. A., Mazzoleni A. P. (2007). Analysis and design for no-spin tethered satellite retrieval. *J. Guid. Control. Dyn.*, **30,** 1516—1519. https://doi.org/10.2514/1.25390
21. Peters T. V., Francisco José, Valero Briz, Olmos Diego Escorial, Lappas V., Jakowski P., Gray I., Tsourdos A., Biesbroek H. R. (2018). Attitude Control Analysis of Tethered De-orbiting *Acta Astronautica*, **146**, 316—331. https://doi.org/10.1016/j.actaastro.2018.03.016
22. Rupp C. C., Kissel R. R. (1978). *Tetherline system for orbiting satellites*. U. S. Patent No. 4083520, April II, 1978, Int. Cl. B. 64 G 1/100, US Cl. 244/167; 244/161
23. Rupp C. C., Laue J. H. (1978). Shuttle/Tethered Satellite System. *J. Astronaut. Sci.,* **26**, 1—17.
24. Stadnyk K., Ulrich S. (2020). Validating the Deployment of a Novel Tether Design for Orbital Debris Removal. *JSR*, **57**, No. 6. https://doi.org/10.2514/1.A34781
25. Steindl A., Troger H. (2003). Optimal control of deployment of a tethered subsatellite. *Nonlinear Dyn.*, **31**, 257—274. https://doi.org/10.1023/A:1022956002484
26. Steiner W., Steindl A., Troger H. (1995). Center manifold approach to the control of a tethered satellite system, *Appl. Math. Comput.*, **70**, 315—327. https://doi.org/10.1023/A:1022956002484
27. Sun Guanghui, Zhu Z. H. (2014). Fractional-Order Tension Control Law for Deployment of Space Tether System. *J. Guid. Control. Dyn.,* **37**, No. 6, 157—167. https://doi.org/ 10.2514/1.G000496
28. Sun Guanghui, Zhu Z. H. (2014). Fractional order tension control for stable and fast tethered satellite retrieval. *Acta Astronautica*, **104**, No. 11, 304—312. https://doi.org/10.1016/j.actaastro.2014.08.012
29. Swet C. J. (1970). *Method for deployment and stabilizing orbiting structures*. U.S. Patent Office No. 3532298, Oct. 6, 1970, Int. Cl. B 64 G 1/00, U.S. Cl. 244-1.
30. Tian H., Li A., Wang Yu., Wang C. (2023). Underactuated Attitude Tracking Control of Tethered Spacecraft for Deployment and Spin-up. *Advs in Space Res.*, **71**, No. 11. https://doi.org/10.1016/j.asr.2023.01.052
31. Tirop P., Jingrui Zh. (2019). Review of Control Methods and Strategies of Space Tether Satellites. *Amer. J. Traffic and Transportation Engineering,* **4**, No. 5, 137—148. https://doi.org/ 10.11648/j.ajtte.20190405.11
32. Wang Ch., Zabolotnov Yu. M. (2017). Control over the deployment of an orbital tether system of great length. *Vestnik of Samara Univ. Aerospace and Mechanical Engineering*, **16**, No. 2, 7—17. https://doi.org/ 10.18287/2541-7533-2017-16-2-7-17
33. Wen Hao, Zhu Z. H., Jin D. P., Hu Haiyan (2016). Space Tether Deployment Feedback Control with Explicit Tension Constraint and Saturation Function. *J. Guid. Control. Dyn*., **39**, No. 4, 1—6. https://doi.org/ 10.2514/1.G001356
34. Williams P. (2008). Deployment/retrieval optimization for flexible tethered satellite systems. *Nonlinear Dyn.*, **52**, 159—179. https://doi.org/10.1007/s11071-007-9269-3
35. Xu R., Özgüner Ümit (2008). Sliding mode control of a class of underactuated systems. *Automatica*, **44**, No. 1, 233—241. https://doi.org/10.1016/j.automatica.2007.05.014
36. Yu B. S., Huang Z., Geng L. L., Jin D. P. (2019). Stability and ground experiments of a spinning triangular tethered satellite formation on a low earth orbit. *Aerospace Sci. and Technology,* **92**, No. 9, 595—604. https://doi.org/10.1016/j.ast.2019.06.012
37. Yu B. S., Wen H., Jin D. P. (2018). Review of deployment technology for tethered satellite systems. *Acta Mech. Sinica*, **34,** No. 4, 754—768. https://doi.org/ 10.1007/s10409-018-0752-5
38. Zakrzhevskii A. E. (2016). Method of Deployment of a Space Bodies tether with Alignment it to the Local Vertical. Patent of UkraineUA 111298, u 2016 03712 from 10.11.15*, Bul. "Promyslova vlasnist",* **21**, 1—4.
39. Zhang K., Lu K., Gu X., Fu C., Zhao S. (2022). Dynamic Behavior Analysis and Stability Control of Tethered Satellite Formation Deployment. *Sensors*, **22**, 62. https://doi.org/10.3390/s22010062
40. Zhang F., Huang P. (2019). A novel underactuated control scheme for deployment/retrieval of space tethered system. *Nonlinear Dyn*., **95**, 3465—3476. https://doi.org/10.1007/s11071-019-04767-3

Стаття надійшла до редакції 10.09.2024 *Received 10.09.2024*
Після доопрацювання 26.09.2024 *Revised 26.09.2024*
Прийнято до друку 27.09.2024 *Accepted 27.09.2024*

Ч. Ван[1], проф.
https://orcid.org/ 0000-0002-1358-7731
E-mail: wangcq@nwpu.edu.cn
О. Є. Закржевський[2], д-р техн. наук, проф., провід. наук. співроб.
https://orcid.org/0000-0003-2106-2086

[1]Північно-західний університет 1
127 YouyiXilu, Xi'an 710072 Shaanxi, Китай
[2]Інститут космічних досліджень Національної академії наук України та Державного космічного агентства України
Проспект Академіка Глушкова 40, корп. 4/1, Київ-187, Україна, 03680

ПРОГРАМНЕ КЕРУВАННЯ ДОДАТКОВИМ РОЗГОРТАННЯМ КОСМІЧНОЇ ЗВ'ЯЗКИ ІЗ ЗБЕРІГАННЯМ ЇЇ ПОЧАТКОВОЇ ВЕРТИКАЛЬНОЇ ОРІЄНТАЦІЇ

Об'єкт цього дослідження — космічна зв'язка двох тіл, з'єднаних безмасовим тросом. Мета дослідження — побудова програмного керування режимом збільшення довжини попередньо розгорнутої космічної зв'язки із збереженням її початкової вертикальної орієнтації. Для цього використовуються рівняння руху зв'язки змінної довжини, записані у сферичних координатах. Побудовано програмне керування довжиною зв'язки, яке забезпечує необхідну зміну її кінетичного моменту під впливом сил гравітаційного поля. Новизна результатів дослідження полягає в новому підході до побудови керування малопривідними механічними системами, у яких кількість каналів керування менша за кількість ступенів свободи. Тут вдається побудувати таке керування довжиною зв'язки, яке дозволяє керувати її рухом і кутом тангажу, використовуючи лише один канал керування — зміна довжини зв'язки. Для цього використовується пасивна, але керована дія на зв'язку гравітаційного моменту. Щоб досягти такого ефекту, пропонується накладати обмеження на рух зв'язки по тангажу, які формально зменшують кількість ступенів свободи системи. Це дозволяє реалізувати заданий режим руху при керуванні тільки за ступенем свободи, що залишився. Вид таких обмежень визначається з огляду на фізичні міркування. Внаслідок врахування всіх вимог, що пред'являються до режиму додаткового розгортання, вдається побудувати закон зміни кута тангажу за часом, що описується степеневим рядом восьмого порядку. Проведено детальне чисельне дослідження впливу параметрів режиму, таких як тривалість розгортання та передбачувана форма закону зміни кута тангажу за часом, на довжину розгорнутої зв'язки та характер її поведінки у процесі розгортання. Наведено чисельний приклад застосування розробленого методу. Чисельне моделювання режиму здійснюється в рамках інтегрування завдання Коші для рівнянь Гілла — Клогессі — Уайтшіра. Проведено кількісну оцінку похибок чисельного моделювання. Результати обчислень проілюстровано графічно.

Ключові слова: *космічна зв'язка, розгортання, керування, зміна довжини, вертикальне положення, малопривідні системи*.